Toxicology in Vitro 73 (2021) 105134

Contents lists available at ScienceDirect

Toxicology in Vitro

journal homepage: www.elsevier.com/locate/toxinvit

Novel indirect co-culture of immortalised hepatocytes with monocyte derived macrophages is characterised by pro-inflammatory cytokine networks

Florian Padberg [a,b,*], Tessa Höper [a], Sebastian Henkel [c], Dominik Driesch [c], Andreas Luch [a,b], Sebastian Zellmer [a]

[a] German Federal Institute for Risk Assessment (BfR), Department of Chemical and Product Safety, Max-Dohrn Straße 8-10, 10589 Berlin, Germany
[b] Department of Biology, Chemistry, Pharmacy, Institute of Pharmacy, Freie Universität Berlin, Arnimallee 22, 14195 Berlin, Germany
[c] BioControl Jena GmbH, Hans-Knöll-Straße 6, 07745 Jena, Germany

ARTICLE INFO

Keywords:
Co-culture
Fa2N-4
Monocyte derived macrophages
Cytokine correlation network
Acute phase

ABSTRACT

The liver is composed of different cell populations. Interactions of different cell populations can be investigated by a newly established indirect co-culture system consisting of immortalised primary human hepatocytes and human monocyte derived macrophages (MDMs). Using the time-dependent cytokine secretion of the co-cultures and single cultures, correlation networks (including the cytokines G-CSF, CCL3, MCP-1, CCL20, FGF, TGF-β1, GM-CSF, IL-8 IL-6, IL-1β, and IL-18) were generated and the correlations were validated by application of IL-8 and TNF-α-neutralising antibodies. The data reveal that IL-8 is crucial for the interaction between hepatocytes and macrophages *in vitro*. In addition, transcriptome analyses showed that a change in the ratio between macrophages and hepatocytes may trigger pro-inflammatory signalling pathways of the acute phase response and the complement system (release of, *e.g.*, certain cyto- and chemokines). Using diclofenac and LPS showed that the release of cytokines is increasing with higher ratios of MDMs. Altogether, we could demonstrate that the current co-culture system is better suited to mirror the *in vivo* situation when compared to previously established co-culture systems composed of HepG2 and differentiated THP-1 cells. Further, our data reveal that the cytokine IL-8 is crucial for the interaction between hepatocytes and macrophages *in vitro*.

1. Introduction

The liver is one of the largest organs in the human body (Abdel-Misih and Bloomston, 2010). It consists of parenchymal cells (hepatocytes) and a variety of non-parenchymal cell populations such as Kupffer cells, stellate cells and endothelial cells (Kmiec, 2001).

Primary hepatocytes are well suited for the investigation of substance-specific metabolic effects. However, liver cell physiology and metabolism are characterised by large inter-individual variations and during *in vitro* cultivation cellular de-differentiation and changes of metabolic capacities occur within days (Soldatow et al., 2013). Such inter-individual differences can be excluded by using hepatic cell lines. However, these cell lines usually originate from an intravital tumour environment and thus may have altered metabolic activities (Wilkening et al., 2003).

The hepatic Fa2N-4 cell line represents an SV-40 immortalised, non-tumorigenic primary human cell line (Mills et al., 2004). Fa2N-4 cells are able to metabolise drugs like diclofenac (DCN), due to the expression and activity of cytochrome P450-dependent monooxygenases (CYP) 2C9 (Mills et al., 2004; Ripp et al., 2006) and CYP3A4, or UDP-

Abbreviations: CC 15%, physiological co-culture; CC 50%, pro inflammatory co-culture; MDM, blood monocyte derived macrophage; HepG2/THP-1, indirect co-cultivation of HepG2 and differentiated THP-1; Fa2N-4/MDM, indirect co-cultivation of Fa2N-4 and MDM cells; αIL-8, anti-interleukin 8 antibodies; AMB, adalimumab; HGF, hepatocyte growth factor; TGF-α, transforming growth factor α; IL, interleukin; TGF-β1, transforming growth factor β1; CCL20, chemokine (C—C motif) ligand 20; CCL3, chemokine (C—C motif) ligand 3; FGF, fibroblast growth factor; GM-CSF, granulocyte-macrophage colony-stimulating factor; MCP-1, monocyte chemoattractant protein 1.

* Corresponding author at: German Federal Institute for Risk Assessment Department, Chemical and Product Safety, Max-Dohrn-Strasse 8-10, 10589 Berlin, Germany.

E-mail address: florian.padberg@bfr.bund.de (F. Padberg).

https://doi.org/10.1016/j.tiv.2021.105134
Received 11 November 2020; Received in revised form 28 January 2021; Accepted 25 February 2021
Available online 2 March 2021

glucuronosyltransferases (UGT) 2B7 and UGT1A9 (Hariparsad et al., 2008). In this context, the expression, inducibility, and activity of CYP1A2, CYP2C9, and CYP3A4 were shown to be comparable between Fa2N-4 and primary hepatocytes (Hariparsad et al., 2008; Mills et al., 2004). In contrast to HepaRG cells, Fa2N-4 cells can be used immediately and no differentiation time of 2–4 weeks is required (Aninat et al., 2006; Gripon et al., 2002). Furthermore, while HepaRG cells originate from a female hepatocarcinoma (Aninat et al., 2006), Fa2N4 cells have a non-tumorigenic origin (Mills et al., 2004).

Kupffer cells are the largest population of tissue macrophages in the liver (Dixon et al., 2013) and play an important role during drug induced liver injury (DILI) (Ju and Reilly, 2012), liver regeneration (Michalopoulos, 2017) and drug metabolism (Ding et al., 2004) to name a few physiological processes. The interaction between hepatocytes, Kupffer cells and infiltrating macrophages is relevant for substance specific hepatotoxicity. In general, liver macrophages, such as Kupffer cells, appear to express markers of different macrophage lineages simultaneously (Guillot and Tacke, 2019). In the physiological human liver, a large inter-individual variability in the ratio of Kupffer cells to hepatocytes (average = 14.5 ± 9.1%) has been reported (Brouwer et al., 1988). Similarly, a range of 8–12% has been described by Gebhardt (1992). Kupffer cells can bind and incorporate proteins, foreign particles, bacteria, yeasts and viruses *via* endocytosis (Wardle, 1987). However, for the operability of *in vitro* models, it should be considered that the availability of primary Kupffer cells is limited and subject to a large inter-individual variability (Wu et al., 2020). Following a metabolic or toxic damage of liver tissue, a massive infiltration of blood mononuclear cells (PBMC), which differentiate into macrophages, occurs (Tacke and Zimmermann, 2014).

Many studies have shown that the *in vitro* co-cultivation of hepatocytes and Kupffer cells (or Kupffer cell-like models) can be used to characterise tissue responses upon exposure to hepatotoxic substances (Granitzny et al., 2017; Rose et al., 2016; Wewering et al., 2017b). Melino et al. (2012) were able to show that hepatocytes responded to secreted factors from differentiated THP-1 cells.

Thus, HepG2 cells are converted into an "inflammatory phenotype" (based on transcriptomic data) while growing in THP-1 conditioned medium (Melino et al., 2012). Indirect co-cultivation of HepG2 and differentiated THP-1 cells (HepG2/THP-1) is a useful *in vitro* approach to identify substances responsible for drug induced liver injury and to discriminate DILI from non-DILI substances (Granitzny et al., 2017; Padberg et al., 2020). Furthermore, HepG2/THP-1 co-culture can help to characterise the causative mechanisms of hepatotoxicity. An important effect of ketoconazole is the induction of an NRF2-mediated oxidative stress response that could be identified in HepG2/THP-1 co-culture (Wewering et al., 2017b). Other data also showed that primary co-cultures consisting of hepatocytes and Kupffer cells in direct contact show specific DILI-trovafloxacin dependent hepatotoxic effect. The hepatotoxic effect is indicated by the alteration of interleukin (IL)-6 and tumour necrosis factor α (TNF-α) levels and CYP3A metabolic capacity (Rose et al., 2016). A recently described *in vitro* co-culture model composed of non-differentiated PBMCs in combination with HepG2 allows an identification of DILI-inducing drugs (Oda et al., 2021). Results from pro-inflammatory *in vitro* models are also known from animal models. It has been shown that moderate inflammation *in vivo* is induced by low doses of lipopolysaccharides (LPS). This lowers the threshold for adverse effects and allows the identification of DILI substances (Buchweitz et al., 2002; Deng et al., 2006; Zou et al., 2009). Since LPS is modified by Kupffer cells, which affects its toxicity, and subsequently degraded by hepatocytes (Treon et al., 1993), it is important to consider not only hepatocytes in the elucidation of compound-specific effects.

In this study we investigated a novel indirect co-culture system, based on Fa2N-4 cells in combination with blood monocyte derived macrophages (MDMs), without a LPS induced inflammation. To simulate the differences between physiological and inflammatory conditions, different Fa2N-4 to MDM ratios of 15% (Brouwer et al., 1988) and 50% were used. The ratio of 50% represent a more than three-fold increase in MDM cell numbers, which has been detected in inflammatory processes of the portal region of human liver (Karakucuk et al., 1989). With these two co-culture systems, time dependent cytokine secretion and alterations of the transcriptome were investigated. The release of cytokines, as well as the phosphorylation status of acute phase associated transcription factor p38 mitogen-activated protein kinase (p38) were determined. Based on the cytokine data, correlation networks were generated using statistical methods. The robustness was studied by using interleukin 8 neutralising antibodies (αIL-8) and the TNF-α neutralising drug Adalimumab (AMB, EMEA/H/C/004475). Furthermore, the effects of DCN and LPS on the cytokine secretion was studied using single and co-cultures with 15% and 50% MDMs.

2. Materials and methods

All methods were carried out according to the manufacturer's protocol. Only modifications are described below.

2.1. Chemicals and antibodies

All chemicals were purchased from Sigma-Aldrich (Taufkirchen, Germany) unless stated otherwise. Dulbecco's phosphate-buffered saline (DPBS) was a product of PAN-Biotech (Aidenbach, Germany). AMB was purchased from Selleck chemicals (BIOZOL, Eching, Germany) and αIL-8 was a product of R&D Systems (Bio-Techne GmbH, Wiesbaden-Nordenstadt, Germany). The complete list of antibodies is given in table S1.

2.2. Cell culture

All following cell cultivations were conducted under treatment with 0.1% dimethyl sulfoxide (DMSO), including solvent controls. All consumables were purchased from TPP (Trasadingen, Switzerland). Microscopic images were taken with an Observer.A1 microscope (LD Plan Neoflua 40×/0.60) from Zeiss (Jena, Germany). Cell cultivation and incubation was performed at 37 °C and 5% CO_2. Penicillin (100 U/ml), 100 µg/ml streptomycin, and 2 mM L-glutamine were added to all cell culture media. Further additives are listed in the cultivation conditions of the individual cells below.

2.3. Hepatocyte cultures

The SV-40 immortalised hepatocytes (Fa2N-4) were purchased from SEKISUI-XenoTech (tebu-bio, Offenbach, Germany). After thawing, Fa2N-4 cells were seeded at a density of 2×10^5 cells per cm^2 and cultivated in Williams E (PAN-Biotech, Aidenbach, Germany) containing 10% (*v*/v) FCS, 100 nM dexamethasone, and 10 µg/ml recombinant human insulin. After 4 h the culture medium was replaced by Williams E containing 100 nM dexamethasone and 10 µg/ml recombinant human insulin for 24 h.

2.4. Monocyte isolation and differentiation into macrophages (MDMs)

Human buffy coats were obtained from anonymised donors, with their consent (votum of the ethics committee: EA4/071/13), from the blood bank (Deutsches Rotes Kreuz, Berlin, Germany). PBMCs were isolated from buffy coats based on the Ficoll® Plaque Plus density gradient centrifugation (450 xg, 35 min, 20 °C). Then, PBMCs were collected at the interphase, followed by three washing steps and a centrifugation at 200 xg with autoMACS Running Buffer (Miltenyi Biotec, Bergisch Gladbach, Germany) at 4 °C to carefully remove the thrombocytes. Monocytes were separated due to the adhesion-properties of the cells. Therefore, the PBMCs were resuspended in RPMI (PAN-Biotech, Aidenbach, Germany) containing 10% (*v*/*v*) FCS and incubated for 1 h at a density of 0.8×10^6 cells per cm^2. After careful

removal of all non-adhered cells, differentiation to MDMs was started using RPMI containing 10% (*v/v*) FCS and 25 ng/ml macrophage-colony-stimulating factor (M-CSF) over six days with a medium change every two days. After the differentiation, all non-adherent cells were removed by washing with DPBS. The MDMs were detached using 10 mM EDTA in DPBS for 30 min at 4 °C.

2.5. Co-cultivation

MDMs were seeded either into the well directly (for the single-cultivation) or into the Falcon® cell culture inserts (VWR, Darmstadt, Germany) for the co-cultivation using Williams E medium, supplemented with 100 nM dexamethasone and 10 μg/ml recombinant human insulin. The 50% and 15% MDMs corresponded to a density of 1×10^5 and 0.3×10^5 cells per cm^2, respectively. After 24 h, the media of MDMs and Fa2N-4 was replaced with Williams E supplemented with 10 μg/ml recombinant human insulin and the MDMs containing cell culture inserts were inserted into the Fa2N-4 culture well. This represents the time point 0. Culture medium with 0.1% DMSO was used as control and cultivated alike to the samples.

2.6. HepG2/THP-1 co-cultivation

HepG2 and THP-1 cells were grown in RPMI supplemented with 10% (v/v) FCS. Single culture THP-1 cells were supplemented additionally with 1 mM sodium pyruvate and 10 mM Hepes. The co-culture was established using Falcon® cell culture inserts (VWR, Darmstadt, Germany) according to Wewering et al. (2017a). HepG2 cells were seeded at a density of 1.3×10^5 cells per cm^2. THP-1 cells were differentiated by 100 nM phorbol 12-myristat 13-acetat (PMA) for 24 h and were seeded at a density of 0.65×10^5 cells (corresponding to a density of 50%) or 0.2×10^5 (representing a density of 15%) per cm^2.

2.7. Cytotoxicity testing

Cytotoxicity was assessed by measuring the activity of the adenylate kinase (AK) in the supernatant using the ToxiLight™ assay (Lonza, Basel, Switzerland). LDH activity in the supernatant was measured using the Cytotoxicity Detection Kit (Roche, Basel, Switzerland). In addition, the MTT Assay was performed according to Mosmann (1983) followed by cell lysis with DMSO. All values were corrected for the DMSO (0.1%) solvent controls.

2.8. RNA isolation procedure

RNA was isolated using the NucleoSpin® RNA Kit (Machery-Nagel, Düren, Germany) according to the manufacturer's protocol.

2.9. Microarray analyses

All samples (RNA integrity number (RIN) >8.5) were analysed using a Human Clariom™ S Assay (Applied Biosystems, Foster City, CA, USA). Further information is provided in the supplementary section. Microarray data have been deposited in the Gene Expression Omnibus (GEO) database, www.ncbi.nlm.nih.gov/geo (accession no. GSE156627).

2.10. Flow-cytometry analyses

FACS-buffer (1% FCS, 0.2 mM EDTA in DPBS) was used for all washing and incubation steps at 4 °C. After staining with LIVE/DEAD™ Fixable Near-IR Dead Cell Stain Kit (Thermo Scientific, Waltham, MA, USA) the cells were fixed with Roti®-Histofix 4% (Roth, Karlsruhe, Germany) for 10 min. The functional antibody or the corresponding isotype controls were diluted in FACS-buffer, applied to the cells and incubated at 4 °C for 15 min. Fluorescence intensities were measured with the FACS Aria III (BD Biosciences, Heidelberg, Germany) with the following settings: PE channel: 585/42 nm, FITC channel: 530/30, APC channel: 660/20, BV421 channel: 450/40, Alexa Fluor 700 channel: 730/45, PerCP channel: 695/23, live/dead channel: 780/60 and generated data were analysed with the FlowJo v 10 software (FlowJo LLC, Ashland, OR, USA).

2.11. Cytokine measurements

Cytokines in the supernatant were quantified using the Cytokine LEGENDplex™ system (Biolegend, San Diego, CA, USA), including the Inflammation Panel 1 (IL-1β, TNF-α, MCP-1, IL-6, IL-8, IL-10, IL-12, IL-18) and the Custom Human Assay (TGF-β1, GM-CSF, G-CSF, FGF, CCL3, CCL20, HGF, TGF-α). The results were analysed using LEGENDplex™ 8.0 software (Biolegend, San Diego, CA, USA).

2.12. Western blot analysis

Cells were lysed at 4 °C in RIPA buffer (50 mM Tris/HCl (pH 7.4), 159 mM NaCl, 1 mM EDTA, 1% Igepal®, 0.25% sodium deoxycholate) supplemented with a protease inhibitor cocktail (Merck, Darmstadt, Germany), composed of 200 μM phenylmethylsulfonyl fluoride and 1 mM sodium orthovanadate. Protein concentrations were determined with the Pierce™ BCA Protein Assay Kit (Thermo Scientific, Waltham, MA, USA), and equal amounts of protein were applied to SDS-PAGE and, after separation, transferred to nitrocellulose membranes. After binding of primary antibodies (16 h at 4 °C), the secondary antibody (horseradish peroxidase labelled) was added for 1 h, and the staining was visualised with Pierce ECL Substrate (Thermo Fisher Scientific, Waltham, MA, USA) using a ChemiDoc XRS (Bio-Rad, Munich, Germany). The signal intensity was normalised to the loading control β-actin and then the ratio of phosphorylated (P) to total p38 protein was calculated.

2.13. Data pre-processing and analysis

All time-resolved data of cytokine concentrations in the supernatant were used for the correlation network analysis. The correlation uses individual replicates and not mean values since the data are paired over both time points and replicates, *i.e.* for a given time point the values of all cytokines originate from the same sample. Data compilation and network generation were performed using the statistical language and environment R (version 3.6.3) (R Core Team, 2018). In detail, in a first step all values below their lower detection limit were set to the half value of that detection limit. Subsequently, all values were log-transformed. Individual samples were grouped (time point 0 h belonging to all groups) with respect to their conditions *i.e.* to either single or one of the co-cultures later becoming individual networks. In particular, for the MDM culture as well as the co-culture the data of the different macrophage ratios (15% and 50%) were combined. Within these data groups for each pair of cytokines, their correlation coefficients and respective p-values were determined by Spearman rank correlation. The p-values were adjusted according to Benjamini-Hochberg. Subsequently, a filter was applied to all pairwise connections with respect to the p-value (significant for $p \leq 0.05$) as well as the correlation coefficient (threshold of $\varrho \leq -0.2$ and $\varrho \geq 0.6$ according to coefficients' distribution and confidence intervals). The remaining connections after filtering were employed to visualise the respective non-directed correlation networks.

Data shown are based on at least three independent biological replicates. Means, standard deviations and ANOVA p-values followed by Bonferroni correction were calculated with GraphPad Prism 6 (Statcon, Witzenhausen, Germany). The *Z*-scores were calculated and visualised with Perseus Software (Tyanova et al., 2016). The Z-score was based on the mean values of the individual cytokine concentrations (values below their lower detection limit were set to the half value of that detection limit) in the corresponding cultivations. Venn diagrams were created using jvenn (Bardou et al., 2014). Volcano-plots were created using

Transcriptome Analysis Console (TAC), version 4.0.1.36 (Applied Biosystems, Foster City, CA, USA). Significant ($p < 0.05$) gene expressions were analysed using Ingenuity® Pathway Analysis (IPA) software (Qiagen, Aarhus, Denmark). Furthermore, only those pathways embedded in the IPA software, that were assigned to liver and immune cell associated pathways, were included in the analysis.

3. Results

3.1. Macrophage derived monocytes express specific markers

During differentiation, characteristic morphological changes of the round shaped PBMCs to elongated fibroblast-like MDMs became obvious (Fig. 1 A). We determined typical macrophage markers and compared those with markers of T-, B- and dendritic cells. About 26% of the PBMCs were $CD14^+$ monocytes and therefore potential macrophage precursors. Almost all (>90%) MDMs were positive for typical macrophage markers (CD83, CD14, CD86, toll-like receptor 4 (TLR4), human leukocyte antigen-DR isotype (HLA-DR) and CD163). Only 28% of the MDMs were also $CD209^+$, being a marker for dendritic cells and M2 macrophages. Furthermore, $CD3^+$ cells, characteristic for T-cells, were only present before the differentiation of PBMCs (Fig. 1 C). Altogether, these surface markers indicated a successful differentiation of the PBMCs to MDMs. A co-culture system composed of these MDMs and the hepatic cell line Fa2N-4 was then developed. The viability of the two cell populations was found to be unaffected by the co-culture condition, since no increased release of the cytoplasmic marker adenylate kinase (AK) was measurable in the supernatant of the cell culture. Even an increase in the ratio of MDMs from 15% to 50% resulted in no changes of the AK level in the supernatant (Fig. 1 B).

3.2. Culture conditions affect Fa2N-4 gene expression

Next, changes of the Fa2N-4 gene expression in the co-culture (relative to the individual culture) were determined at two different time points (24 h and 48 h) and two different ratios of MDMs (15% and 50%). The physiological conditions were simulated with a co-culture consisting of 15% MDMs (CC 15%) and for inflammatory conditions a co-culture with 50% MDMs (CC 50%) was used.

In general, the total number of differential expressed genes was independent of the number of macrophages (Fig. 2 A). Microarray data indicated that 357 genes were significantly ($p < 0.05$) differentially regulated during physiological co-cultivation (CC 15%) and 419 genes during inflammatory co-cultivation (CC 50%) after 24 h (Fig. 2 B). A prolongation of the cultivation time to 48 h resulted in about 30% more significantly expressed genes in both co-cultures, compared to single cultivated Fa2N-4 cells (Fig. 2 B). Among all genes pro-inflammatory signalling pathways took a central role, especially in the CC 50% after 24 h. Under these conditions, we were able to identify the signalling pathways of the "complement system" and the "acute phase response signalling" (Fig. 2 C) as top two of all regulated pathways. A total of 16 signalling pathways are marked as significantly regulated ($p < 0.05$). The gene lists of exclusively significant genes of the CC 50% (567 genes) after 24 h were used for the pathway analyses. In the CC 50% after 24 h, 18% of significantly regulated genes could be attributed to "complement system signalling" and showed a high probability of regulation ($p < 0.01$). The "acute phase response signalling" was also identified, with lower ratios (up to 9%) but with partially higher probabilities of $p < 0.001$ (Fig. 2 C) and 21% of the expected associated target gene expression. After an incubation time of 48 h we were able to identify other signalling pathways like neuroinflammation and T-helper cell

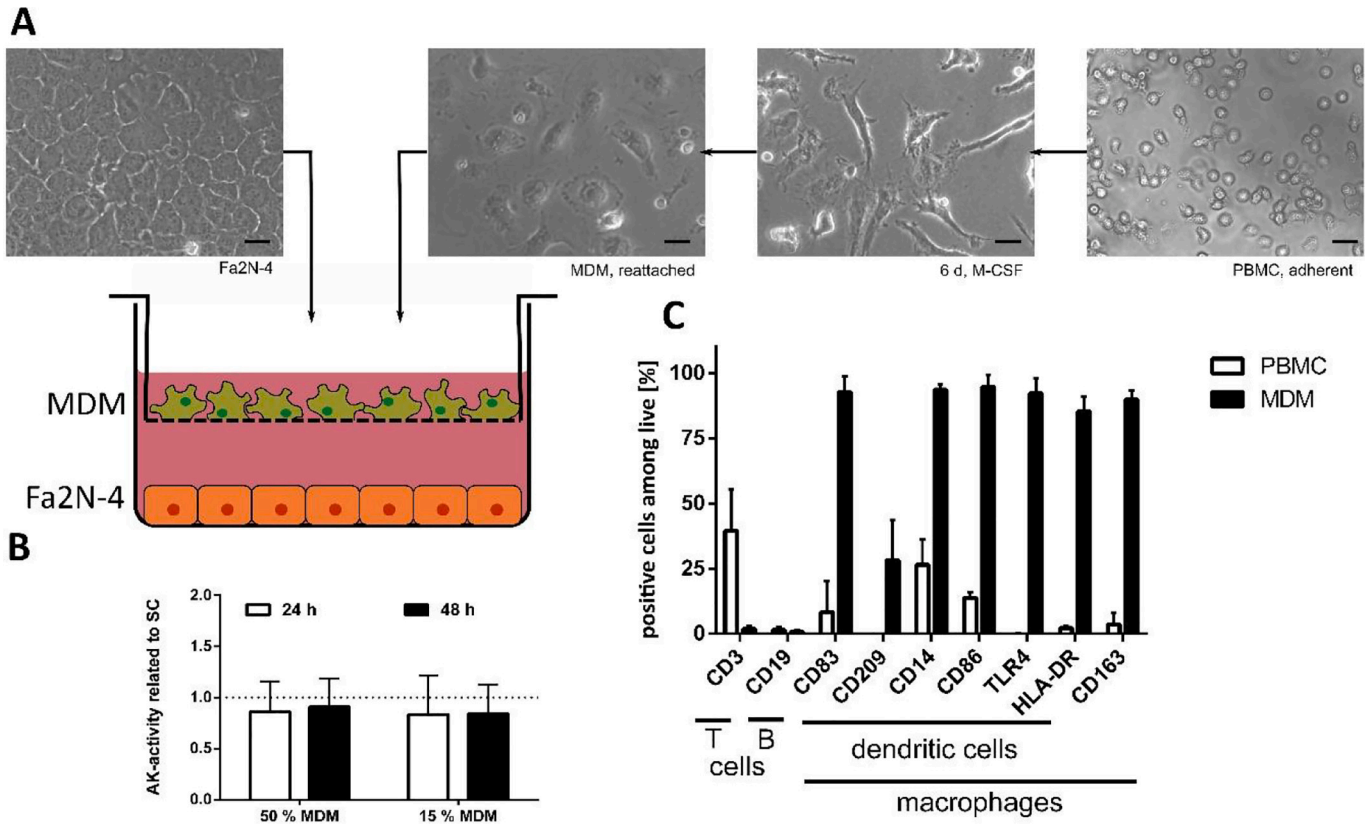

Fig. 1. Set-up of the co-culture, cytotoxicity and expression of cell specific surface markers. **(A)** Images of the Fa2N-4 cells and of the differentiation process from peripheral blood mononuclear cells (PBMC) after 6 d of differentiation with 25 ng/ml of macrophage colony stimulating factor (M-CSF) to monocyte derived macrophages (MDMs). The scale bar denotes 20 μm. **(B)** Toxicity of physiological (15%) and pro-inflammatory (50%) ratios of MDM-to-Fa2N-4 cells were tested. The dotted line represents the reference (single culture, SC) of the adenylate kinase (AK) in the supernatant. **(C)** The presence of CD163, toll-like receptor 4 (TLR4) and human leukocyte antigen - DR isotype (HLA-DR) indicated a successful differentiation of the PBMCs into MDMs. $n = 3$, bars represent mean ± SD.

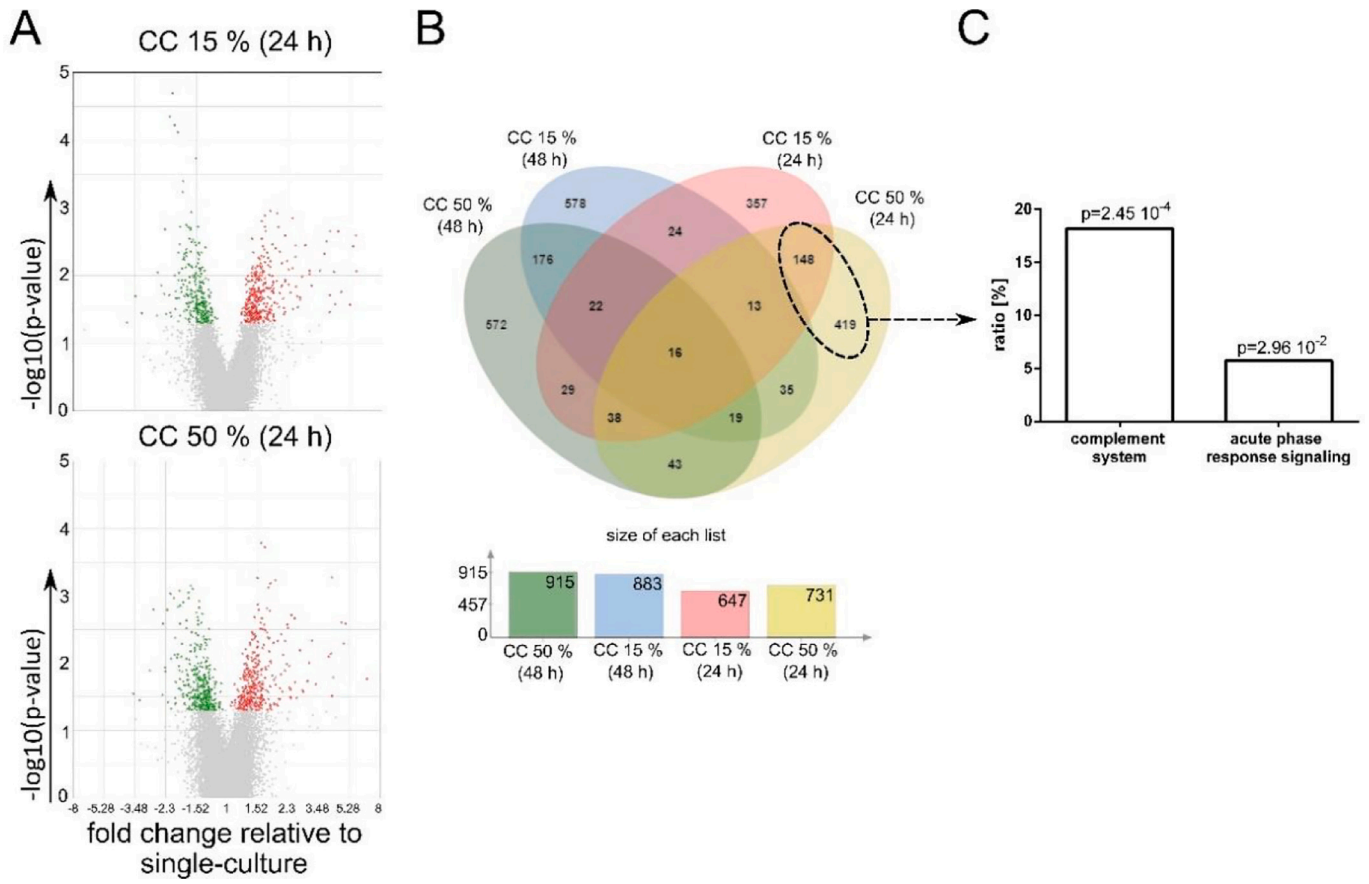

Fig. 2. Microarray analysis reveals time- and MDM-dependent differences in the gene expression of Fa2N-4 cells. Fa2N-4 cells were co-cultivated with monocyte derived macrophages (MDMs). Physiological (CC 15%) and pro-inflammatory (CC 50%) conditions were studied and related to the corresponding single cell culture of Fa2N-4 cells ($n = 3$). (**A**) Volcano-plots included all significantly upregulated (red) and downregulated (green) genes of the CC 15% and CC 50% after 24 h. The significance was set to $p < 0.05$ ($-\log_{10}(p) > 1.3$). (**B**) Venn diagram and the size of each gene list of significantly ($p < 0.05$) expressed genes based on microarray analysis. Different MDM ratios and cultivation times (24 h or 48 h) resulted in specific expression patterns. (**C**) Significantly regulated genes of the pro-inflammatory signalling pathways "complement system" and "acute phase response" in relation to all genes involved (ratio) and their respective p-value (after 24 h) of expressed genes of the CC 50%.

associated pathways. We did not consider these pathways in further analysis, since they were not related to hepatic pathophysiology and contain no or only 9% of the expected associated target gene expressions.

In summary, inflammatory signalling pathways are activated within 24 h during co-cultivation.

3.3. An acute phase transcription factor is phosphorylated

Especially in the CC 50%, our transcriptome analysis indicated a major role for the acute phase response signalling.

Therefore, the phosphorylation of the transcription factor p38 was studied. The relative phosphorylation (P-p38/p38) was 0.8 ± 0.1 in Fa2N-4 cells, 2.0 ± 0.4 in the CC 15% and 1.5 ± 0.3 CC 50% after 4 h of co-cultivation (Fig. 3).

In summary, the indirect co-cultivation of Fa2N-4 and MDM (Fa2N-4/MDM) cells results in the phosphorylation of the transcription factor p38.

3.4. Cytokine secretion depends on the culture conditions

Next, we analysed the time-dependent release of cytokines in the co-cultures (Fig. 4). In contrast to MDMs, secreted cytokines of Fa2N-4 cells accumulated after 48 h of cultivation (Fig. 4 A). The majority of cytokines showed a steep increase in single cell cultivated Fa2N-4 cells and during co-cultivation after 48 h. However, hepatocyte growth factor

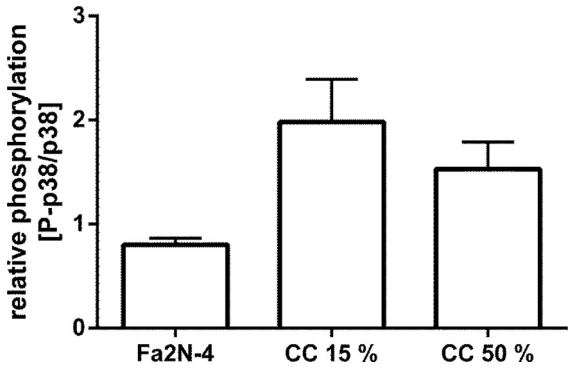

Fig. 3. Semi-quantitative western blot analysis of phosphorylation of the transcription factor p38. Western blot analysis of Fa2N-4 cells with ("CC") and without MDMs after 4 h. Physiological (15%, $n = 3$) and pro-inflammatory (50%, $n = 3$) MDM numbers were used. ($n = 2$). Shown are the mean and the SD of the culture dependent phosphorylation of p38 mitogen-activated protein kinase (p38) in Fa2N-4 cells. Fig. S2 shows a representative blot.

(HGF), transforming growth factor (TGF)-α, TNF-α, IL-10, and IL-12 showed no clear time-dependent accumulation (Fig. 4 A, g, h, j, n, o). In general, co-cultures showed increased absolute levels of cytokine secretion. Among others, the concentration of fibroblast growth factor (FGF) in co-culture reached up to 7532.5 pg/ml in CC 15% after 48 h and

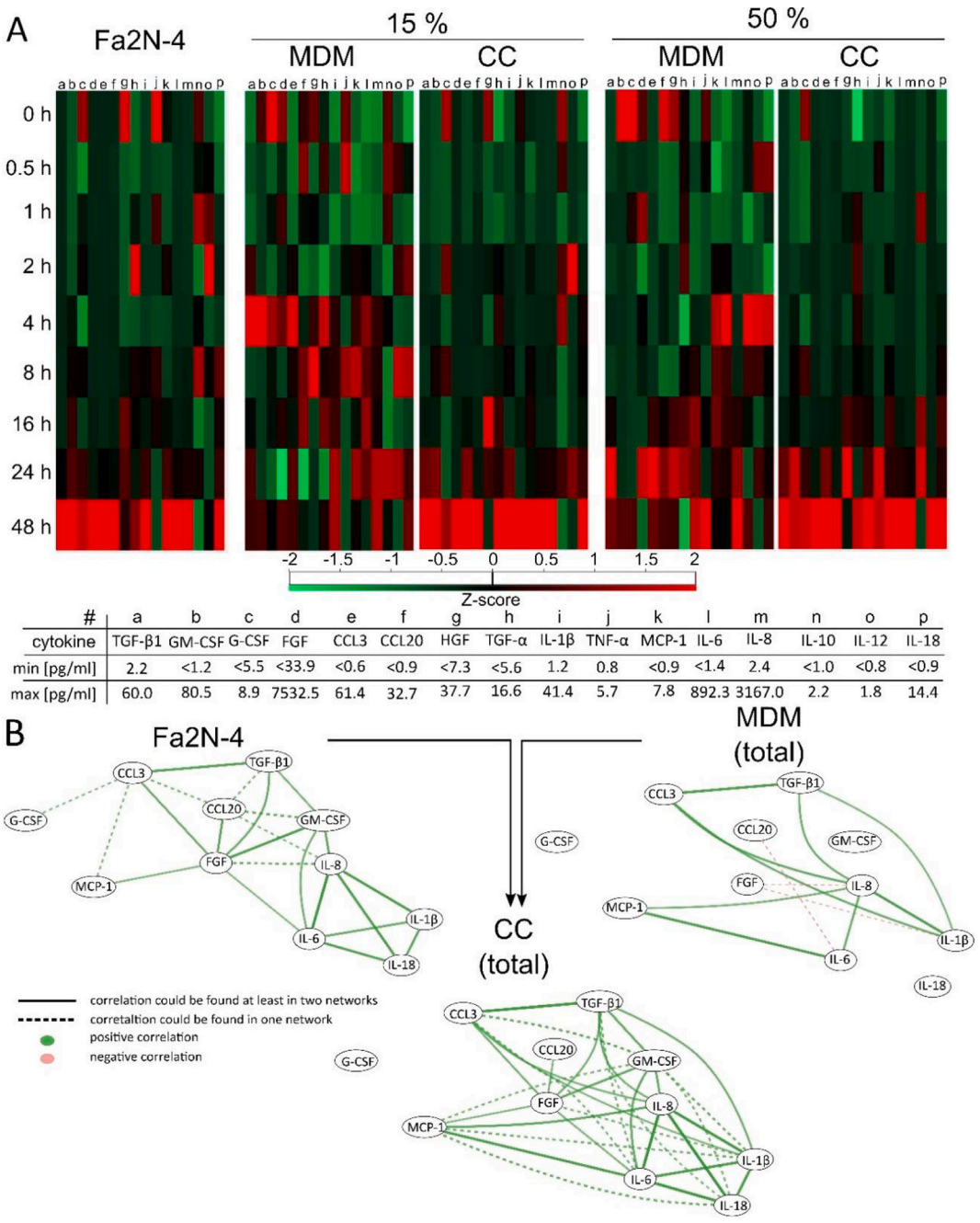

#	a	b	c	d	e	f	g	h	i	j	k	l	m	n	o	p
cytokine	TGF-β1	GM-CSF	G-CSF	FGF	CCL3	CCL20	HGF	TGF-α	IL-1β	TNF-α	MCP-1	IL-6	IL-8	IL-10	IL-12	IL-18
min [pg/ml]	2.2	<1.2	<5.5	<33.9	<0.6	<0.9	<7.3	<5.6	1.2	0.8	<0.9	<1.4	2.4	<1.0	<0.8	<0.9
max [pg/ml]	60.0	80.5	8.9	7532.5	61.4	32.7	37.7	16.6	41.4	5.7	7.8	892.3	3167.0	2.2	1.8	14.4

Fig. 4. Effect of co-culture on cytokine secretion and its temporal progression. Fa2N-4 cells were co-cultivated with monocyte derived macrophages (MDMs) for 48 h. Physiological (15%) and pro-inflammatory (50%) MDM numbers were used. (**A**) Heatmaps of the time-dependent cytokine concentration in the supernatant included the *Z*-score of the means within one row of the heatmap. Letters (a-p) indicate the individual cytokines. Only the lowest (min) and highest (max) cytokine concentrations are shown (complete data are given in table S2). (**B**) The time-dependent concentrations were used for the generation of correlation networks. Solid lines (——) indicate that these correlations occur in the co-culture network and in at least one of the single cultivation networks. Dotted lines (–) identify additional correlations occurring in the respective network. A positive correlation is labelled green and a negative correlation is labelled red. The data were generated from three independent experiments.

IL-8 reached up to 892.3 pg/ml in CC 50% after 48 h. The absolute concentration of IL-6 in the co-culture was 200-fold higher compared to the single cultures with a maximum concentration of 892.3 pg/ml (Fig. 4 A).

In summary, most of the investigated cytokines accumulated in cultures consisting of Fa2N-4 cells only and in the co-cultures of Fa2N-4/MDMs after 48 h (Fig. 4 A).

3.5. Correlation networks visualise the relationship between secreted cytokines

Next, a statistical approach was used to identify significant Spearman correlations (indicated by respective correlation coefficients and p-values) between cytokine concentration values (Fig. 4 B). The co-cultures CC 15% and CC 50% were combined, because it is assumed that the behaviour of each of the single cultures and the co-culture is structurally the same but that the two ratios lead to different inflammatory states represented by respective cytokine concentrations. The

correlation network indicated that the chemokine (C—C motif) ligand (CCL) 20 played a central role in the individual cultivation of Fa2N-4 cells, since correlations exist to five other cytokines: CCL3, FGF, TGF-β1, granulocyte-macrophage colony-stimulating factor (GM-CSF), and IL-8. The secretion of FGF seemed to be also important in the Fa2N-4 associated correlation network. Six FGF-dependent correlations were identified in the Fa2N-4 single cell cultivations and in the co-cultivations with MDMs. While CCL20-FGF showed significant correlation in co-

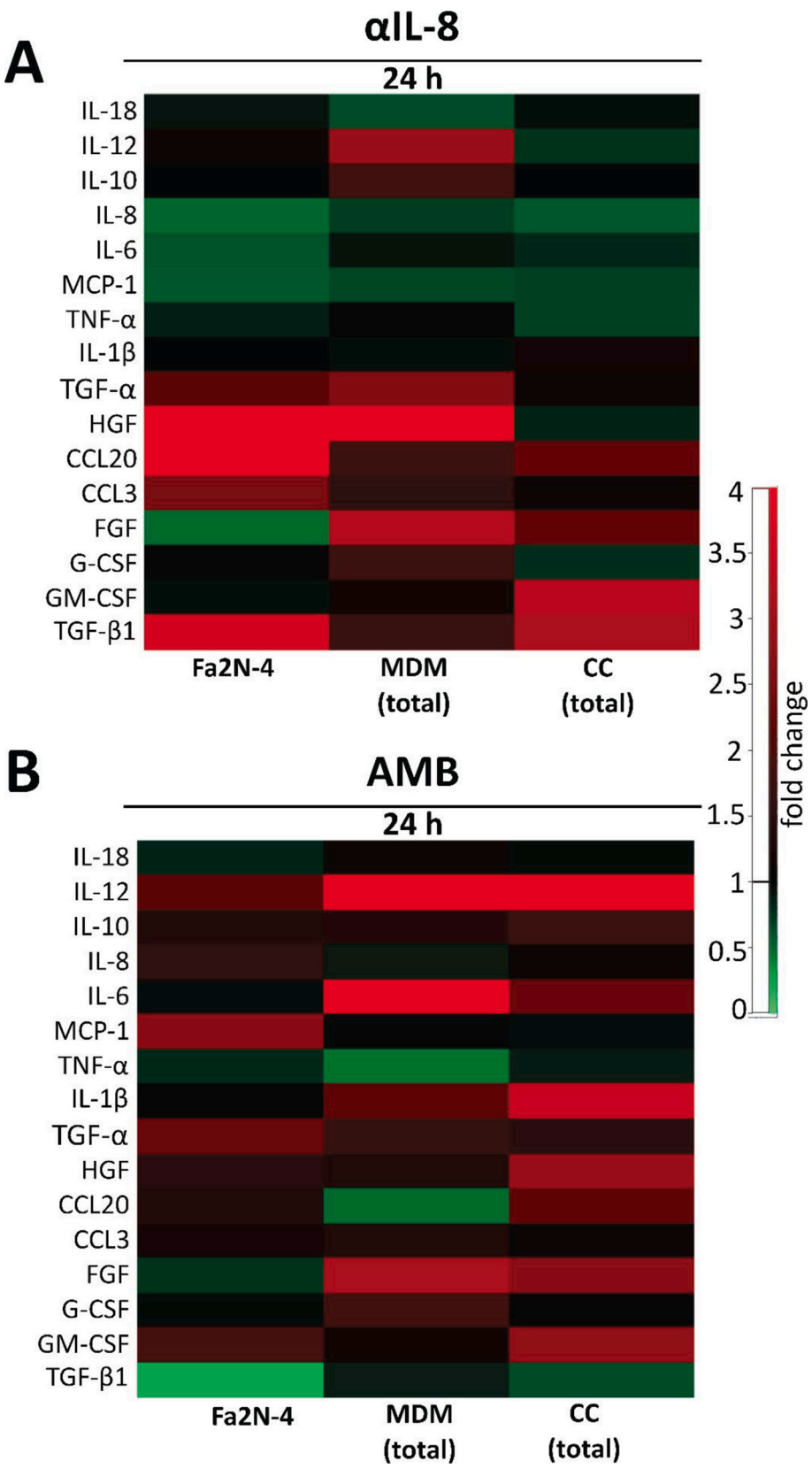

Fig. 5. Analysis of αIL-8- and TNF-α-specific alterations on the cytokine secretion pattern. Fa2N-4 cells were co-cultivated (CC) with monocyte derived macrophages (MDMs) for 24 h. Physiological (15%) and pro-inflammatory (50%) MDM-to-Fa2N-4 ratios were used. All measured cytokine concentrations were related to the corresponding control (fold change) to analyse **(A)** the IL-8 neutralising antibody (αIL-8, 100 ng/ml) specific effect and **(B)** the TNF-α neutralising effect of Adalimumab (AMB, 500 ng/ml).

culture, the central cytokine in this network was IL-8, which was correlated to seven other cytokines. Interestingly, IL-8 differed in terms of correlation between the individual cultures and co-cultivations. However, all of the IL-8 connections in the co-cultivation network could be found in at least one of the single cultivation networks. Among the correlations of IL-8 in the co-cultivation network, the one to IL-6 was the strongest based on its correlation coefficient (table S3). Strikingly, the connection between IL-8 and FGF showed opposing correlation in the individual networks: positive for Fa2N-4 and negative for MDM cells (Fig. 4 B). Further, there were some other connections that showed differences between the MDMs and the co-cultivation network: another change in its direction occurred between FGF and IL-1β. Finally, there were FGF correlations that cannot be found in the MDM network but occur in co-cultivation (FGF-TGF-β1, FGF-CCL3, and FGF-MCP-1).

In summary, cytokine secretion in co-culture was more complex and correlations between the cytokines changed when compared to single cultures. Therefore, the correlation network of the co-culture did not represent a simple merge of the Fa2N-4 and MDM networks but showed additional cytokine interactions between the two cell types.

Since inflammatory processes seemed to dominate after 48 h (Fig. 4), all further investigations were performed at the time point of 24 h of cultivation. To investigate the central role of IL-8 in the co-culture, further studies were conducted in the presence of αIL-8.

3.6. αIL-8 affects the cytokine release

The neutralising antibody αIL-8 was used to investigate the role of IL-8 in the correlation network and to study how its reduction/elimination affects the outcome. For this purpose, we added αIL-8 (100 ng/ml) to all samples. An acute toxic effect of αIL-8 was excluded by analysing the LDH activity in the cell culture supernatant (*c.f.* Fig. S1).

To investigate the effects of αIL-8 treatment on the secreted cytokines, we determined the total cytokine concentration in the supernatant (table S2) after 24 h, which was normalized to the control (Fig. 5A). The αIL-8 treatment led not only to a reduction of the average concentration of IL-8, but also diminished the monocyte chemoattractant protein 1 (MCP-1) in all cultivations (Fig. 5 A). FGF was reduced in the supernatant of Fa2N-4 cells, however the MDM cells secreted more FGF under the influence of αIL-8. Additionally, HGF was secreted only in the single cultures (Fa2N-4 and MDM cells, respectively). In contrast, treatment with αIL-8 induced GM-CSF secretion only in the co-cultivation system. CCL20 secretion due to αIL-8 treatment was detected in the Fa2N-4 cells.

In summary, αIL-8 treatment provoked specific changes in the cytokine secretion pattern, thus supporting the certain role of IL-8 in inflammatory cytokine networks of hepatic cells.

3.7. Adalimumab treatment alters the secretion of cytokines

Adalimumab (AMB) was used to study the effect of a decreased tumour necrosis factor α (TNF-α) concentration on the correlation network.

The concentration of TNF-α after treatment with AMB was in the range of 1.7 pg/ml ± 0.2 to 5.5 pg/ml ± 3.2 after 4 h (data not shown) and in the range of 1.6 pg/ml ± 0.7 to 4.0 pg/ml ± 1.1 after 24 h, respectively. In the untreated cell culture, TNF-α showed no significant correlation to changes of the levels of other cytokines (Fig. 4 B). Upon treatment of the cultures with AMB, a role of TNF-α in the co-culture system could be identified (Fig. 5 B). Twenty-four hours after addition of AMB to the co-culture, an increased secretion of cytokines, present in the afore depicted correlation network (*e.g.* GM-CSF, CCL20, FGF, IL-1β) was determined (up to 3.4-fold) compared to the corresponding controls. In addition, treatment resulted in a reduced IL-6 secretion (0.7-fold) similar to TGF-β1 (0.6-fold) (Fig. 5 B). In the single culture of Fa2N-4 cells, a reduction of TGF-β1 and FGF (0.2-fold and 0.7-fold) occurred, while MCP-1 secretion increased 2.7-fold after 24 h (Fig. 5 B). In the single cultivated MDMs, the cytokine CCL20 decreased (0.5-fold), while the concentration of IL-6 increased (8.6-fold) after 24 h of AMB treatment (Fig. 5 B).

In summary, treatment with the TNF-α neutralising AMB leads to major changes in the cytokine secretion.

3.8. Treatment with diclofenac and lipopolysaccharide leads to changes in cytokine secretion depending on the inflammatory status

The Fa2N-4/MDM were treated with the non-steroidal drug DCN and with LPS. In order to exclude acute toxic effects, 5% of the effective concentration (EC_5) was calculated for DCN, using the MTT assay (Fig. S3) and LPS, using the LDH assay (Fig. S4). Concentrations of 157 μM for DCN and 100 ng/ml for LPS were used in further experiments. Fig. 6 gives an overview of the treatment dependent cytokine secretion of different cultivations. In contrast to the untreated co-cultures (*c.f.* Fig. 4) the drug treatment resulted in a higher release of cytokines.

Fig. 6 summarizes the different co-cultivation conditions in order to compare the treatment-related effects in relation to the inflammatory status (*e.g.* 15% MDMs and 50% MDMs). In general, treatment with 157 μM DCN lead to a reduction in cytokine secretion in the CC 15% compared to the control (Fig. 6 A). Only selected cytokines such as HGF and CCL20 in the single culture of Fa2N-4 as well as TGF-β1 and FGF in the pro-inflammatory co-culture (CC 50%) showed an increase in secretion compared to the control. The pattern is different in LPS treated cultures (Fig. 6 B). After 24 h, a clear increase in secretion of nine cytokine can be detected; most prominently in the pro-inflammatory (CC 50%) co-culture culture. The concentration of the cytokines IL-10, IL-8, IL-6, HGF, CCL3, FGF, and TGF-β1 are higher compared to the control and, except for IL-6 and HGF, also in the corresponding single cultivation of MDMs (MDM 50%).

It can be concluded that the co-culture (CC 15%) under the influence of DCN leads to reduced cytokine secretion, whereas individual cytokines are increasingly secreted in the pro-inflammatory co-cultivation with 50% MDMs. A similar increased cytokine secretion can be observed after LPS treatment of the pro-inflammatory CC 50%.

3.9. Comparison of cytokine profiles in FA2N-4/MDM and HepG2/THP-1 co-cultures

The newly established indirect co-cultivation of Fa2N-4 and MDM (Fa2N-4/MDM) cells was compared with already established similar systems. For this purpose we selected the co-culture model consisting of HepG2 and PMA-differentiated THP-1 (Padberg et al., 2020; Padberg et al., 2019). For better comparability, the HepG2/THP-1 cells were cultivated in similar numbers as the Fa2N-4/MDM cells. Subsequently, the same cytokines were measured in the supernatant at the same time intervals and a correlation network was calculated. In general, HepG2 cells formed a much less complex correlation network of cytokines than Fa2N-4 cells and THP-1 cells form a more complex network compared to MDMs.

Networks for Fa2N-4/MDM and HepG2/THP-1 co-cultivation were based on similar cytokines (Fig. 7 and Fig. 4 B). However, the cytokines TGF-β1, FGF and IL-6 played a minor role in HepG2/THP-1 co-cultivation compared to Fa2N-4/MDM co-cultivation. Yet, correlations of TNF-α and TGF-α were detectable in HepG2/THP-1 co-cultivation (Fig. 7). In addition, HepG2/THP-1 co-cultivation revealed a correlation between interleukin 1β (IL-1β) and interleukin 18 (IL-18). All other correlations were also present in either the THP-1 or the HepG2 single culture networks. In the co-culture the results obtained looked like some sort of addition of the THP-1 and HepG2 networks (Fig. 7). Altogether, the cytokine network found in the Fa2N-4/MDM co-culture (Fig. 4 B) was more complex, compared to the network detected in HepG2/THP-1 co-culture (Fig. 7).

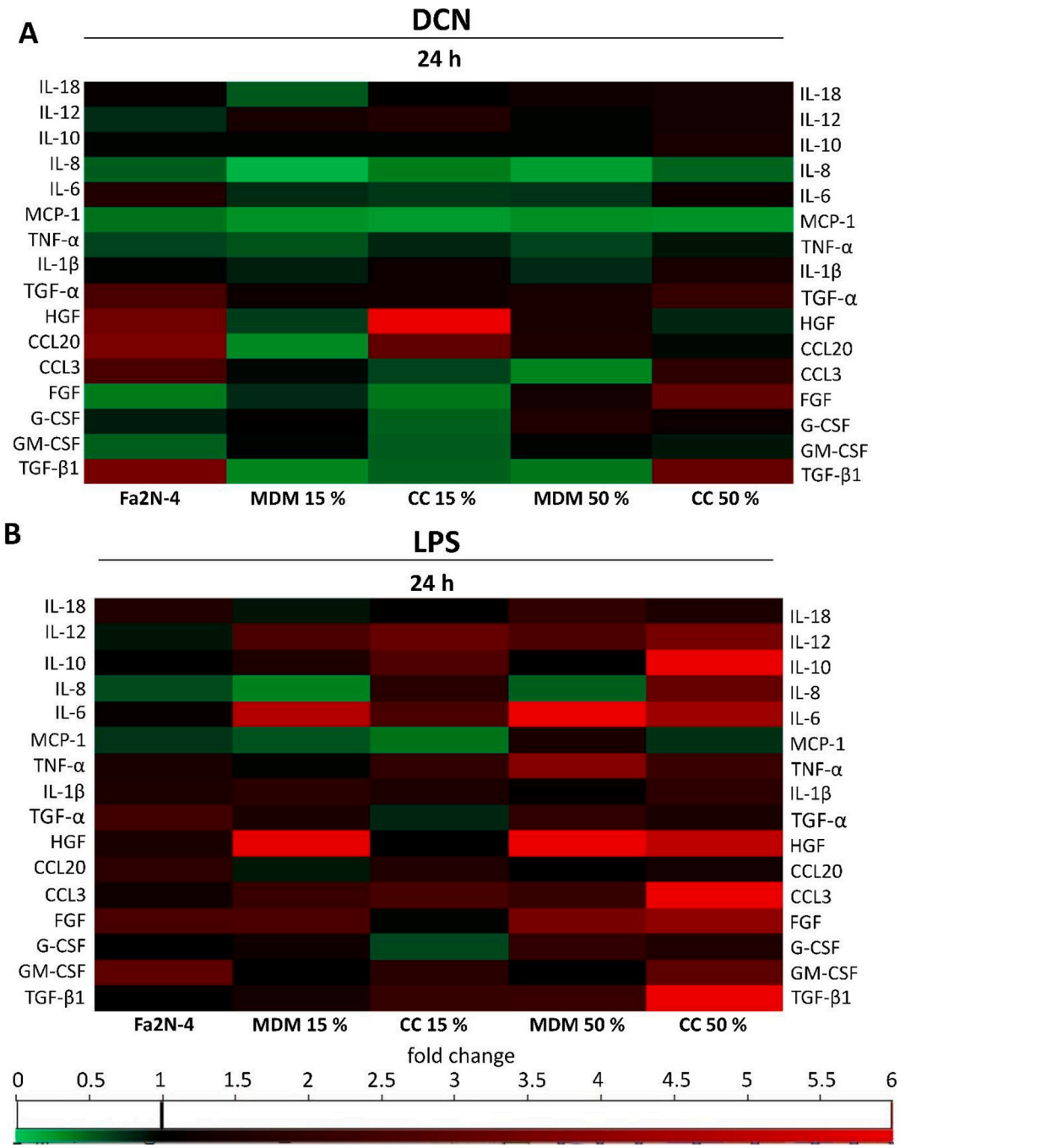

Fig. 6. Analysis of DCN and LPS specific alterations of the cytokine secretion pattern. Fa2N-4 cells were co-cultivated (CC) with monocyte derived macrophages (MDM) for 24 h. Physiological (15%) and pro-inflammatory (50%) MDM to Fa2N-4 ratios were used. All measured cytokine concentrations were related to the corresponding control (fold change) to analyse (**A**) the diclofenac (DCN, 157 μM) and (**B**) lipopolysaccharides (LPS, 100 ng/ml). Data are based on three biological replicates. For visualization a cut-of value of 6-fold was chosen. The particular fold changes are given in table S4.

4. Discussion

A novel co-culture system, consisting of immortalised hepatocytes (Fa2N-4) and MDM cells, has been established. In a first step, the differentiation of MDMs was characterised. Differentiated MDM cells expressed typical surface markers (Bertani et al., 2017; Cao et al., 2005; Lai et al., 2006; Taylor et al., 2004): CD83, CD209, CD14, CD86, TLR4, HLA-DR and CD163 (Fig. 1). However, only 28% of the MDMs were CD209 positive ($CD209^+$, Fig. 1). Among liver cells, Kupffer cells were also reported to be positive for CD209 (Lai et al., 2006). In addition to Kupffer cells, also human anti-inflammatory M2 macrophages (but no pro-inflammatory M1 macrophages) were $CD209^+$ (Buchacher et al., 2015). This indicates that CD209 negative ($CD209^-$) MDMs in this co-culture system might represent the heterogeneity of macrophages migrating into the liver due to an inflammatory response. Thus, this Fa2N-4/MDM system is independent of the limited availability of primary Kupffer cells and primary human hepatocytes. In contrast to the model of Oda et al. (2021) which relies on PBMCs this study consists of differentiated PBMCs (MDMs).

An inflammatory status of cellular systems can improve the detection of adverse chemicals. It is known that modest inflammation during drug therapy lowers the hepatotoxic threshold and leads to adverse effects

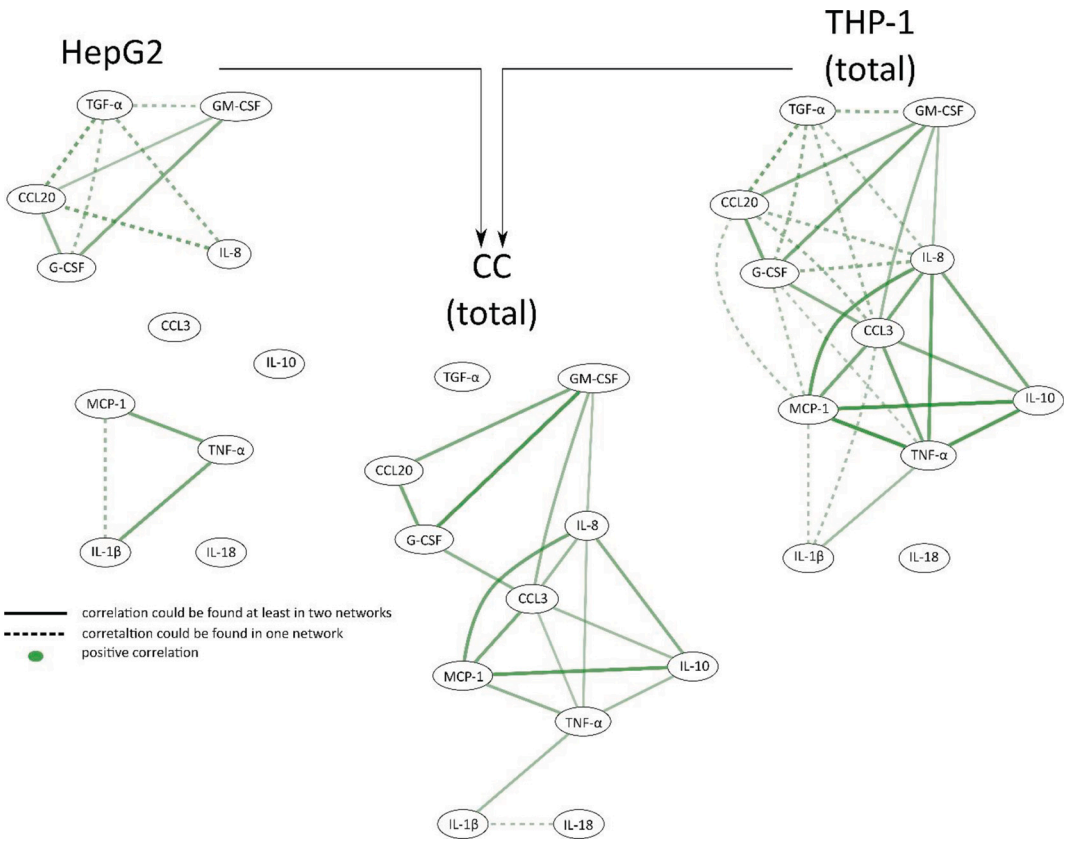

Fig. 7. Correlation network analysis of the HepG2/THP-1 co-cultivation reveals additive effects. HepG2 cells were co-cultivated (CC) with PMA-differentiated THP-1 cells. Physiological (15%) and pro-inflammatory (50%) THP-1 numbers were used. Overall 16 cytokines were measured (given in table S5) at the same time points (0, 0.5, 1, 2, 4, 8, 16, 24 and 48 h) like the Fa2N-4/MDM co- and single cell cultivation (*c.f.* Fig. 4). Solid lines (——) indicate that these correlations occur in the co-cultivation network and in at least one of the single cultivation networks. Dotted lines (–) identify additional correlations occurring in the respective network. $n = 3$.

(Roth and Ganey, 2011). These adverse effect can be reproduced in an animal model by performing co-treatment with low doses of lipopolysaccharides (LPS) (Buchweitz et al., 2002; Deng et al., 2006; Zou et al., 2009). In contrast to several studies, we did not use LPS to simulate an inflammatory environment, but increased the number of MDM cells in the co-culture (CC 50%) and compared these with the "physiological" number of MDMs present (CC 15%). The "physiological" concentration was calculated from data published by (Brouwer et al., 1988), who reported an average of 14.5 ± 9.1% Kupffer cells from seven human liver preparations. To our knowledge, our paper is the first work in which the extent of the pro-inflammatory status depends on the hepatocyte-to-MDM ratio and not on prior substance-specific induction of pro-inflammation. Hence this novel co-culture system allows to study adverse substance effects depending on its inflammatory status.

The number of MDM cells and the total incubation time (24 h or 48 h) affected the gene expression pattern of Fa2N-4 cells (Fig. 2). Independent transcriptome-based pathway analysis of the two different co-cultures (CC 15% and CC 50%, respectively) after 24 h revealed the activation of an acute phase response mainly in the CC 50% culture (Fig. 2 C) which could be confirmed by the phosphorylation of p38 (Fig. 3). Coulouarn et al. (2004) have shown that the gene expression in primary human liver cells correlated with the severity of the acute phase response and supporting our data of the transcriptome-based pathway analysis in connection with the phosphorylation of p38.

It is well known that the secretion of various pro-inflammatory cytokines (*e.g.* IL-6, TNF-α, IL-1β) is part of an acute phase reaction (Ramadori and Christ, 1999). Therefore, we investigated the time course of secreted cytokines (Fig. 4 A) and established a correlation network of these cytokines (Fig. 4 B). Similar to the *in vivo* situation, cytokine secretion in co-culture was more complex compared to single cultivated cells and did not represent the sum of the Fa2N-4 and MDM dependent networks (Fig. 4 B). IL-8 played a central role under co-cultivation conditions, as indicated by seven correlations to other cytokines and an elevated absolute concentration (Fig. 4). In contrast, the previously studied HepG2/THP-1 co-culture systems (Granitzny et al., 2017; Padberg et al., 2020; Wewering et al., 2017b) showed only five correlations of IL-8 to other cytokines (Fig. 7).

In vivo correlations between IL-8, IL-6 and IL-1β, that have been described in the literature (Table 1), occurred only in the Fa2N-4/MDM network and were absent in the HepG2/THP-1 co-culture (using a cut-off value of $p < 0.05$). To validate the *in vitro* cytokine correlations in HepG2/THP-1 and Fa2N-4/MDM networks further, information from literature was retrieved. Table 1 compares the two correlation networks in focus (Fig. 4 B + Fig. 7) with the data found in the literature. The single- and co-cultivation of Fa2N-4 and MDM cells showed more similarities between *in vivo* reported correlation networks (*c.f.* Fig. 4 B) than the co-cultivation of HepG2 and THP-1 cells (Fig. 7). However, Fa2N-4/MDM co-cultivation did not mirror all cytokine profiles reported in the literature. This might be related to the absence of other hepatic cells such as endothelial cells and Ito cells (Brouwer et al., 1988; Gebhardt, 1992) that are present in healthy liver. Furthermore, the concentrations of some cytokines, like TNF-α in Fa2N-4/MDM co-cultures (Table 1 + Fig. 4 B) and IL-6 in HepG2/THP-1 co-cultivations (Table 1 + Fig. 7), were at the lowest level of possible quantification, which also caused the absence of respective nodes and edges in the correlation networks. In addition, the (statistically) absence of correlations between cytokines in the correlation network did not necessarily indicate that there was no biological dependence. The absence might be based on the predefined cut-off value of $p < 0.05$, set in the statistical analysis (*c.f.* Fig. 4 B). This in particular includes cytokines that are present at high concentrations,

Table 1
Comparison of the established correlation network analyses of the co-cultures with literature data. Correlation network analyses of co-cultivations (CC) of Fa2N-4 cells with monocyte derived macrophages (MDMs) and HepG2 cells with PMA-differentiated THP-1 cells (*c.f.*Fig. 4 B + 7) were compared with inflammatory cytokine profiles from the literature. The literature data shown here were based on liver-associated cell types in an inflammatory state (*e.g.* virus infections, exposure to lipopolysaccharide, thioacetamide, carbon tetrachloride or ethanol). Shown were either complete agreement (✓) or at least one agreement ((✓)) of the direct correlations with the cytokine profiles found in the literature. (Denaes et al., 2016; Dong et al., 2019; Dou et al., 2019; Hosel et al., 2009; Mandrekar et al., 2011; Meng et al., 2012; Qin et al., 2012; Seki et al., 2001; Shrivastava et al., 2013; Yang et al., 2010)

Fa2N-4/MDMs			HepG2/THP-1			literature		
Fa2N-4	MDM	CC	HepG2	THP-1	CC	Cytokines	species	reference
(✓)		(✓)	(✓)	(✓)	(✓)	IL-1β, IL-6, TNF-α,TGF-β1	mouse	(Meng et al., 2012)
(✓)		(✓)	(✓)	(✓)	(✓)	IL-1β, IL-6, TNF-α	mouse	(Dong et al., 2019)
(✓)		(✓)	(✓)	(✓)	(✓)	IL-1β, IL-6, IL-10, TNF-α	mouse	(Yang et al., 2010)
✓		✓				IL-1β, IL-6	mouse	(Qin et al., 2012)
(✓)	✓	✓	(✓)	(✓)	(✓)	IL-1β, IL-8, TGF-β1, MCP-1	mouse	(Dou et al., 2019)
(✓)	(✓)	(✓)	(✓)	(✓)	(✓)	IL-1β, IL-6, TNF-α, MCP-1	mouse	(Mandrekar et al., 2011)
(✓)		(✓)	(✓)	(✓)	(✓)	IL-1β, IL-6, TNF-α, CCL3	mouse	(Denaes et al., 2016)
✓	(✓)	✓				IL-1β, IL-6, IL-8	human	(Hosel et al., 2009)
✓		✓			✓	IL-1β, IL-18	human	(Shrivastava et al., 2013)
(✓)		(✓)			(✓)	IL-1β, IL-12, IL-18	mouse	(Seki et al., 2001)

but have no correlation to any other cytokine. As already mentioned, IL-8 is of particular importance in the Fa2N-4/MDM co-culture and potential correlations can be confirmed by the literature (Table 1).

In general, IL-8 and the corresponding receptor C-X-C motif chemokine receptor 1 (CXCR1) are responsible for the recruitment of macrophages and neutrophils (Ishida et al., 2006). We investigated the role of IL-8 in our co-culture system by using the neutralising antibody αIL-8 (Fig. 5 A). The heatmap (Fig. 5 A) showed that the concentration of IL-8 decreased in the presence of αIL-8, as expected. Some correlations predicted by the correlation network were confirmed. A decrease in IL-8 resulted in a reduced secretion of FGF in single cultured Fa2N-4 cells, supporting the prediction that both are positive correlated (Fig. 4 B). In MDM cells, the decrease of IL-8 resulted in an increased secretion of FGF, supporting the predicted negative correlation. Furthermore, the correlation network (Fig. 4 B) indicated that MCP-1 correlates positively with IL-8 in co-cultures and in single cultivated MDMs. Reduction of IL-8 by the treatment with αIL-8 resulted in a decrease of MCP-1 in co-cultures and single-cultivated MDM cells (Fig. 5 A). This positive correlation could be supported by expression data from the literature. An increase in the gene expression of MCP-1 and IL-8 has been previously shown in co-cultures of HepaRG cells with PBMCs (Beringer et al., 2019).

The depletion of IL-8 also resulted in some unexpected findings, which did not match the predictions of the correlation network. A positive correlation existed between IL-8 and CCL20 in FA2N-4 single cultures (Fig. 4 B). Despite this positive correlation, the CCL20 concentration increased after lowering the level of IL-8 (Fig. 5 A).

Besides the influence of IL-8 we investigated the effect of TNF-α on cytokine secretion using AMB. AMB is a monoclonal TNF-α neutralising IgG1 antibody used for the treatment of patients with rheumatoid arthritis (French et al., 2016). It is capable of inducing DILI (Ghabril et al., 2013) and thus has been listed in the DILIrank dataset (Chen et al., 2016).

Treatment with AMB resulted in several changes of the cytokine concentrations. Obviously, IL-6 was reduced in co-culture after treatment with AMB (Fig. 5 B). The connection between IL-6 and TNF-α has been described before: In a mouse model, TNF-α in the serum peaked at 1.5 h and IL-6 after 4 h after LPS injection (Hong et al., 2009). This temporal relationship of TNF-α and IL-6 after LPS treatment was also shown in cultured rat hepatocytes (Saad et al., 1995). Furthermore, a positive correlation between IL-6 and TGF-β1 is likely, since murine fibroblasts showed an IL-6 induced expression of TGF-β1 (Luckett-Chastain and Gallucci (2009)). Therefore, the predictions of the correlation network are supported by literature. The negative correlation of CCL20 and IL-6 in the single culture of MDM cells was confirmed, since an increase of IL-6 increased resulted in a decrease of TGF- β1 (Fig. 4 B). In addition, the positive correlation of TGF-β1 and FGF in single cultured Fa2N-4 cells (Fig. 4 B) was confirmed, since both decreased after the AMB induced reduction of TNF-α (Fig. 5 B). Similar to the αIL-8 treatments, not all correlations of the cytokine network could be validated *via* an AMB induced decrease of TNF-α. A reduction of the FGF concentration in single culture of Fa2N-4 cells should lead to a reduction of MCP-1 concentration according to the correlation network (Fig. 4 B). However, this MCP-1 reduction did not occur after AMB treatment (Fig. 5 B).

After 24 h of AMB treatment (Fig. 5 B) three additional positive correlations could be verified in co-culture with regard to FGF levels (with CCL20, IL-1β and GM-CSF, *c.f.*Fig. 4 B). In summary, we could confirm several correlation predictions. With regard to the effect of AMB, the secretion of FGF and IL-6 led to changes in other associated cytokine secretions exclusively under co-cultivation condition.

Besides the general neutralisation of TNF-α, AMB is known as a potential DILI inducing substance (Frider et al., 2013). Another DILI inducing substance is DCN (Boelsterli, 2003), although the structure and mode of action are completely different. Fig. 6 A gives an overview of the changed cytokine secretion as a result of DCN treatment depending on the cultivation set-up. The simulation of a healthy cell ratio (CC 15%) leads to a reduction of most cytokine secretion after DCN treatment

when compared to control. This confirms the known anti-inflammatory effect of DCN (Skoutakis et al., 1988). Another more differentiated cytokine secretion pattern was present in the pro-inflammatory CC 50%. The down-regulated cytokine secretion of IL-8, MCP-1 and GM-CSF in particular follows the postulated positive correlation based upon network analyses (Fig. 4 B). The detectable upregulation of TGF-β1 and FGF secretion in the CC 50% after DCN treatment compared to the control was also predicted by the network analyses. However, DCN treatment can also show that other measured cytokines such as HGF and TGF-α play a role in co-cultivation although they do not show dependencies in the correlation networks. The reason for this is the generally low secretion of these cytokines in the absence of stimulating drugs or xenobiotics.

To investigate the induction of the cytokine secretion in more detail, cultures were treated with LPS (Fig. 6 B). Especially the pro-inflammatory CC 50% responded to LPS treatment with an increased secretion of IL-12, IL-10, IL-8, IL-6, HGF, CCL3, FGF, GM-CSF and TGF-β1 compared to the untreated control (Fig. 6 B). Most of these cytokines are mapped in the correlation network. In general, secretion of cytokines in the LPS-treated pro-inflammatory CC 50% system is known from the early and late response of monocytes and macrophages. IL-6, IL-8 and IL-12 can be attributed to the early response (up to 6 h after treatment) and IL-10, TGF-β1 and GM-CSF (up to 24 h after treatment) are known from the late response (Rossol et al., 2011). Furthermore, an increase in the HGF concentration in the supernatant of the CC 50% is detectable after the LPS treatment. In a rat model, HGF is known to prevent LPS-induced liver failure (Kaido et al., 1997). This indicates that our co-culture system shows a response to LPS and, in addition, supports the reported protective effect of HGF.

In summary, reduction of TNF-α by AMB treatment and the reduction of IL-8 by αIL-8 treatment (Fig. 5) resulted in decreases of several correlated cytokines, indicating the validity of the network (Fig. 4 B). The treatment with DCN or LPS shows, that the ratio of MDMs affects the amount of cytokines released. The data demonstrate that co-cultivation of Fa2N-4 and MDMs creates a complex cytokine correlation network. This novel Fa2N-4/MDM co-culture shows a high similarity to published *in vivo* data.

5. Conclusion

A successful co-cultivation of an immortalised hepatic cell line (Fa2N-4) with monocyte derived macrophages (MDMs) was established. This resulted in the release of pro-inflammatory cytokines. It triggers pathways such as an acute phase response and the complement system. The concentrations of the cytokines released differed between co- and individually cultured cells as well as between a corresponding model consisting of HepG2 and differentiated THP-1 cells. A network of cytokine interactions showed that IL-8 plays a central role in the network. Changes in the IL-8 level affected numerous other cytokines, which allowed to validate the central role of IL-8. In addition, treatment with the TNF-α neutralising antibody (AMB), DCN and LPS showed that the resulting changes in cytokine secretion could be partially predicted by the correlation network. Especially the treatment of DCN and LPS proved that the CC 50% simulates a pro-inflammatory status with an further increase of cytokine secretion. During the AMB exposure FGF, likewise to IL-6, was an important soluble factor.

Declaration of Competing Interest

The authors declare that they have no known competing financial interests or personal relationships that could have appeared to influence the work reported in this paper.

The authors declare the following financial interests/personal relationships which may be considered as potential competing interests:

Acknowledgements

We would like to thank Dr. J. Kugler and Dr. P. Tarnow for the helpful discussions and proofreading. The financial support of the BfR through intramural grants 1322-655 and 1329-003 is gratefully acknowledged.

Appendix A. Supplementary data

Supplementary data to this article can be found online at https://doi.org/10.1016/j.tiv.2021.105134.

References

Abdel-Misih, S.R., Bloomston, M., 2010. Liver anatomy. Surg. Clin. N. Am. 90, 643–653.
Aninat, C., Piton, A., Glaise, D., Le Charpentier, T., Langouët, S., Morel, F., Guguen-Guillouzo, C., Guillouzo, A., 2006. Expression of cytochromes P450, conjugating enzymes and nuclear receptors in human hepatoma HepaRG cells. In: Drug Metabolism and Disposition: The Biological Fate of Chemicals, 34, pp. 75–83.
Bardou, P., Mariette, J., Escudié, F., Djemiel, C., Klopp, C., 2014. Jvenn: an interactive Venn diagram viewer. BMC Bioinformatics 15, 293.
Beringer, A., Molle, J., Bartosch, B., Miossec, P., 2019. Two phase kinetics of the inflammatory response from hepatocyte-peripheral blood mononuclear cell interactions. Sci. Rep. 9, 8378.
Bertani, F.R., Mozetic, P., Fioramonti, M., Iuliani, M., Ribelli, G., Pantano, F., Santini, D., Tonini, G., Trombetta, M., Businaro, L., Selci, S., Rainer, A., 2017. Classification of M1/M2-polarized human macrophages by label-free hyperspectral reflectance confocal microscopy and multivariate analysis. Sci. Rep. 7, 8965.
Boelsterli, U.A., 2003. Diclofenac-induced liver injury: a paradigm of idiosyncratic drug toxicity. Toxicol. Appl. Pharmacol. 192, 307–322.
Brouwer, A., Barelds, R.J., de Leeuw, A.M., Blauw, E., Plas, A., Yap, S.H., van den Broek, A.M., Knook, D.L., 1988. Isolation and culture of Kupffer cells from human liver. Ultrastructure, endocytosis and prostaglandin synthesis. J. Hepatol. 6, 36–49.
Buchacher, T., Ohradanova-Repic, A., Stockinger, H., Fischer, M.B., Weber, V., 2015. M2 polarization of human macrophages favors survival of the intracellular pathogen chlamydia pneumoniae. PLoS One 10, e0143593.
Buchweitz, J.P., Ganey, P.E., Bursian, S.J., Roth, R.A., 2002. Underlying endotoxemia augments toxic responses to chlorpromazine: is there a relationship to drug idiosyncrasy? J. Pharmacol. Exp. Ther. 300, 460–467.
Cao, W., Lee, S.H., Lu, J., 2005. CD83 is preformed inside monocytes, macrophages and dendritic cells, but it is only stably expressed on activated dendritic cells. Biochemical J. 385, 85–93.
Chen, M., Suzuki, A., Thakkar, S., Yu, K., Hu, C., Tong, W., 2016. DILIrank: the largest reference drug list ranked by the risk for developing drug-induced liver injury in humans. Drug Discov. Today 21, 648–653.
Coulouarn, C., Lefebvre, G., Derambure, C., Lequerre, T., Scotte, M., Francois, A., Cellier, D., Daveau, M., Salier, J.-P., 2004. Altered gene expression in acute systemic inflammation detected by complete coverage of the human liver transcriptome. Hepatology 39, 353–364.
Denaes, T., Lodder, J., Chobert, M.N., Ruiz, I., Pawlotsky, J.M., Lotersztajn, S., Teixeira-Clerc, F., 2016. The cannabinoid receptor 2 protects against alcoholic liver disease via a macrophage autophagy-dependent pathway. Sci. Rep. 6, 28806.
Deng, X., Stachlewitz, R.F., Liguori, M.J., Blomme, E.A.G., Waring, J.F., Luyendyk, J.P., Maddox, J.F., Ganey, P.E., Roth, R.A., 2006. Modest inflammation enhances diclofenac hepatotoxicity in rats: role of neutrophils and bacterial translocation. J. Pharmacol. Exp. Ther. 319, 1191.
Ding, H., Tong, J., Wu, S.C., Yin, D.K., Yuan, X.F., Wu, J.Y., Chen, J., Shi, G.G., 2004. Modulation of Kupffer cells on hepatic drug metabolism. World J. Gastroenterol. 10, 1325–1328.
Dixon, L.J., Barnes, M., Tang, H., Pritchard, M.T., Nagy, L.E., 2013. Kupffer cells in the liver. Compr Physiol 3, 785–797.
Dong, X., Liu, J., Xu, Y., Cao, H., 2019. Role of macrophages in experimental liver injury and repair in mice. Exp. Ther. Med. 17, 3835–3847.
Dou, L., Shi, X., He, X., Gao, Y., 2019. Macrophage phenotype and function in liver disorder. Front. Immunol. 10, 3112.
French, J.B., Bonacini, M., Ghabril, M., Foureau, D., Bonkovsky, H.L., 2016. Hepatotoxicity associated with the use of anti-TNF-α agents. Drug Saf. 39, 199–208.
Frider, B., Bruno, A., Ponte, M., Amante, M., 2013. Drug-induced liver injury caused by adalimumab: a case report and review of the bibliography. Case Rep. Hepatol. 2013, 406901.
Gebhardt, R., 1992. Metabolic zonation of the liver: regulation and implications for liver function. Pharmacol. Ther. 53, 275–354.
Ghabril, M., Bonkovsky, H.L., Kum, C., Davern, T., Hayashi, P.H., Kleiner, D.E., Serrano, J., Rochon, J., Fontana, R.J., Bonacini, M., 2013. Liver injury from tumor necrosis factor-α antagonists: analysis of thirty-four cases. Clin. Gastroenterol. Hepatol. 11, 558–564 e553.
Granitzny, A., Knebel, J., Muller, M., Braun, A., Steinberg, P., Dasenbrock, C., Hansen, T., 2017. Evaluation of a human in vitro hepatocyte-NPC co-culture model for the prediction of idiosyncratic drug-induced liver injury: a pilot study. Toxicol. Rep. 4, 89–103.

Gripon, P., Rumin, S., Urban, S., Le Seyec, J., Glaise, D., Cannie, I., Guyomard, C., Lucas, J., Trepo, C., Guguen-Guillouzo, C., 2002. Infection of a human hepatoma cell line by hepatitis B virus. Proc. Natl. Acad. Sci. U. S. A. 99, 15655–15660.
Guillot, A., Tacke, F., 2019. Liver macrophages: old dogmas and new insights. Hepatol Commun 3, 730–743.
Hariparsad, N., Carr, B.A., Evers, R., Chu, X., 2008. Comparison of immortalized Fa2N-4 cells and human hepatocytes as in vitro models for cytochrome P450 induction. In: Drug Metabolism and Disposition: The Biological Fate of Chemicals, 36, pp. 1046–1055.
Hong, Y.-H., Chao, W.-W., Chen, M.-L., Lin, B.-F., 2009. Ethyl acetate extracts of alfalfa (Medicago sativa L.) sprouts inhibit lipopolysaccharide-induced inflammation in vitro and in vivo. J. Biomed. Sci. 16, 64.
Hosel, M., Quasdorff, M., Wiegmann, K., Webb, D., Zedler, U., Broxtermann, M., Tedjokusumo, R., Esser, K., Arzberger, S., Kirschning, C.J., Langenkamp, A., Falk, C., Buning, H., Rose-John, S., Protzer, U., 2009. Not interferon, but interleukin-6 controls early gene expression in hepatitis B virus infection. Hepatology 50, 1773–1782.
Ishida, Y., Kondo, T., Kimura, A., Tsuneyama, K., Takayasu, T., Mukaida, N., 2006. Opposite roles of neutrophils and macrophages in the pathogenesis of acetaminophen-induced acute liver injury. Eur. J. Immunol. 36, 1028–1038.
Ju, C., Reilly, T., 2012. Role of immune reactions in drug-induced liver injury (DILI). Drug Metab. Rev. 44, 107–115.
Kaido, T., Yamaoka, S., Seto, S.-I., Funaki, N., Kasamatsu, T., Tanaka, J., Nakamura, T., Imamura, M., 1997. Continuous hepatocyte growth factor supply prevents lipopolysaccharide-induced liver injury in rats. FEBS Lett. 411, 378–382.
Karakucuk, I., Dilly, S.A., Maxwell, J.D., 1989. Portal tract macrophages are increased in alcoholic liver disease. Histopathology 14, 245–253.
Kmiec, Z., 2001. Cooperation of liver cells in health and disease. Adv. Anat. Embryol. Cell Biol. 161, 1–151.
Lai, W.K., Sun, P.J., Zhang, J., Jennings, A., Lalor, P.F., Hubscher, S., McKeating, J.A., Adams, D.H., 2006. Expression of DC-SIGN and DC-SIGNR on human sinusoidal endothelium: a role for capturing hepatitis C virus particles. Am. J. Pathol. 169, 200–208.
Luckett-Chastain, L.R., Gallucci, R.M., 2009. Interleukin (IL)-6 modulates transforming growth factor-beta expression in skin and dermal fibroblasts from IL-6-deficient mice. Br. J. Dermatol. 161, 237–248.
Mandrekar, P., Ambade, A., Lim, A., Szabo, G., Catalano, D., 2011. An essential role for monocyte chemoattractant protein-1 in alcoholic liver injury: regulation of proinflammatory cytokines and hepatic steatosis in mice. Hepatology 54, 2185–2197.
Melino, M., Gadd, V.L., Walker, G.V., Skoien, R., Barrie, H.D., Jothimani, D., Horsfall, L., Jones, A., Sweet, M.J., Thomas, G.P., Clouston, A.D., Jonsson, J.R., Powell, E.E., 2012. Macrophage secretory products induce an inflammatory phenotype in hepatocytes. World J. Gastroenterol. 18, 1732–1744.
Meng, F., Wang, K., Aoyama, T., Grivennikov, S.I., Paik, Y., Scholten, D., Cong, M., Iwaisako, K., Liu, X., Zhang, M., Osterreicher, C.H., Stickel, F., Ley, K., Brenner, D.A., Kisseleva, T., 2012. Interleukin-17 signaling in inflammatory, Kupffer cells, and hepatic stellate cells exacerbates liver fibrosis in mice. Gastroenterology 143, 765–776 e763.
Michalopoulos, G.K., 2017. Hepatostat: liver regeneration and normal liver tissue maintenance. Hepatology 65, 1384–1392.
Mills, J.B., Rose, K.A., Sadagopan, N., Sahi, J., de Morais, S.M., 2004. Induction of drug metabolism enzymes and MDR1 using a novel human hepatocyte cell line. J. Pharmacol. Exp. Ther. 309, 303–309.
Mosmann, T., 1983. Rapid colorimetric assay for cellular growth and survival: application to proliferation and cytotoxicity assays. J. Immunol. Methods 65, 55–63.
Oda, S., Uchida, Y., Aleo, M.D., Koza-Taylor, P.H., Matsui, Y., Hizue, M., Marroquin, L.D., Whritenour, J., Uchida, E., Yokoi, T., 2021. An in vitro coculture system of human peripheral blood mononuclear cells with hepatocellular carcinoma-derived cells for predicting drug-induced liver injury. Arch. Toxicol. 95, 149–168.
Padberg, F., Tarnow, P., Luch, A., Zellmer, S., 2019. Minor structural modifications of bisphenol a strongly affect physiological responses of HepG2 cells. Arch. Toxicol. 93, 1529–1541.
Padberg, F., Hering, H., Luch, A., Zellmer, S., 2020. Indirect co-cultivation of HepG2 with differentiated THP-1 cells induces AHR signalling and release of pro-inflammatory cytokines. Toxicol. in Vitro 68, 104957.
Qin, H., Holdbrooks, A.T., Liu, Y., Reynolds, S.L., Yanagisawa, L.L., Benveniste, E.N., 2012. SOCS3 deficiency promotes M1 macrophage polarization and inflammation. J. Immunol. 189, 3439–3448.
R Core Team, . R: A language and environment for statistical computing. URL. https://www.R-project.org/. R Foundation for Statistical Computing, Vienna, Austria.
Ramadori, G., Christ, B., 1999. Cytokines and the hepatic acute-phase response. Semin. Liver Dis. 19, 141–155.
Ripp, S.L., Mills, J.B., Fahmi, O.A., Trevena, K.A., Liras, J.L., Maurer, T.S., de Morais, S. M., 2006. Use of immortalized human hepatocytes to predict the magnitude of clinical drug-drug interactions caused by CYP3A4 induction. In: Drug Metabolism and Disposition: The Biological Fate of Chemicals, 34, pp. 1742–1748.
Rose, K.A., Holman, N.S., Green, A.M., Andersen, M.E., LeCluyse, E.L., 2016. Co-culture of hepatocytes and Kupffer cells as an in vitro model of inflammation and drug-induced hepatotoxicity. J. Pharm. Sci. 105, 950–964.
Rossol, M., Heine, H., Meusch, U., Quandt, D., Klein, C., Sweet, M.J., Hauschildt, S., 2011. LPS-induced cytokine production in human monocytes and macrophages. Crit. Rev. Immunol. 31, 379–446.
Roth, R.A., Ganey, P.E., 2011. Animal models of idiosyncratic drug-induced liver injury—current status. Crit. Rev. Toxicol. 41, 723–739.
Saad, B., Frei, K., Scholl, F.A., Fontana, A., Maier, P., 1995. Hepatocyte-derived interleukin-6 and tumor-necrosis factor alpha mediate the lipopolysaccharide-induced acute-phase response and nitric oxide release by cultured rat hepatocytes. Eur. J. Biochem. 229, 349–355.
Seki, E., Tsutsui, H., Nakano, H., Tsuji, N., Hoshino, K., Adachi, O., Adachi, K., Futatsugi, S., Kuida, K., Takeuchi, O., Okamura, H., Fujimoto, J., Akira, S., Nakanishi, K., 2001. Lipopolysaccharide-induced IL-18 secretion from murine Kupffer cells independently of myeloid differentiation factor 88 that is critically involved in induction of production of IL-12 and IL-1beta. J. Immunol. 166, 2651–2657.
Shrivastava, S., Mukherjee, A., Ray, R., Ray, R.B., 2013. Hepatitis C virus induces interleukin-1beta (IL-1beta)/IL-18 in circulatory and resident liver macrophages. J. Virol. 87, 12284–12290.
Skoutakis, V.A., Carter, C.A., Mickle, T.R., Smith, V.H., Arkin, C.R., Alissandratos, J., Petty, D.E., 1988. Review of diclofenac and evaluation of its place in therapy as a nonsteroidal Antiinflammatory agent. Drug Intelligence Clin. Pharma. 22, 850–859.
Soldatow, V.Y., Lecluyse, E.L., Griffith, L.G., Rusyn, I., 2013. In vitro models for liver toxicity testing. Toxicol Res (Camb) 2, 23–39.
Tacke, F., Zimmermann, H.W., 2014. Macrophage heterogeneity in liver injury and fibrosis. J. Hepatol. 60, 1090–1096.
Taylor, P.R., Martinez-Pomares, L., Stacey, M., Lin, H.H., Brown, G.D., Gordon, S., 2004. Macrophage receptors and immune recognition. Annu. Rev. Immunol. 23, 901–944.
Treon, S.P., Thomas, P., Broitman, S.A., 1993. Lipopolysaccharide (LPS) processing by Kupffer cells releases a modified LPS with increased hepatocyte binding and decreased tumor necrosis factor-alpha stimulatory capacity. Proc. Soc. Exp. Biol. Med. 202, 153–158.
Tyanova, S., Temu, T., Sinitcyn, P., Carlson, A., Hein, M.Y., Geiger, T., Mann, M., Cox, J., 2016. The Perseus computational platform for comprehensive analysis of (prote) omics data. Nat. Methods 13, 731.
Wardle, E.N., 1987. Kupffer cells and their function. Liver 7, 63–75.
Wewering, F., Jouy, F., Caliskan, S., Kalkhof, S., von Bergen, M., Luch, A., Zellmer, S., 2017a. Hepatic co-cultures in vitro reveal suitable to detect Nrf2-mediated oxidative stress responses on the bladder carcinogen o-anisidine. Toxicol. in Vitro 40, 153–160.
Wewering, F., Jouy, F., Wissenbach, D.K., Gebauer, S., Blüher, M., Gebhardt, R., Pirow, R., von Bergen, M., Kalkhof, S., Luch, A., Zellmer, S., 2017b. Characterization of chemical-induced sterile inflammation in vitro: application of the model compound ketoconazole in a human hepatic co-culture system. Arch. Toxicol. 91, 799–810.
Wilkening, S., Stahl, F., Bader, A., 2003. Comparison of primary human hepatocytes and hepatoma cell line Hepg2 with regard to their biotransformation properties. In: Drug Metabolism and Disposition: The Biological Fate of Chemicals, 31, pp. 1035–1042.
Wu, X., Hollingshead, N., Roberto, J., Knupp, A., Kenerson, H., Chen, A., Strickland, I., Horton, H., Yeung, R., Soysa, R., Crispe, I.N., 2020. Human liver macrophage subsets defined by CD32. Front. Immunol. 11, 2108.
Yang, H., Hreggvidsdottir, H.S., Palmblad, K., Wang, H., Ochani, M., Li, J., Lu, B., Chavan, S., Rosas-Ballina, M., Al-Abed, Y., Akira, S., Bierhaus, A., Erlandsson-Harris, H., Andersson, U., Tracey, K.J., 2010. A critical cysteine is required for HMGB1 binding to toll-like receptor 4 and activation of macrophage cytokine release. Proc. Natl. Acad. Sci. U. S. A. 107, 11942–11947.
Zou, W., Devi, S.S., Sparkenbaugh, E., Younis, H.S., Roth, R.A., Ganey, P.E., 2009. Hepatotoxic interaction of sulindac with lipopolysaccharide: role of the hemostatic system. Toxicol. Sci. 108, 184–193.